

Peculiarities of the pyroelectric current generated using a LiNbO₃ single crystal driven by low-frequency sinusoidal temperature variation

A. Oleinik^{1,*}, M. Gilts¹, P. Karataev², A. Klenin¹, A. Kubankin^{1,3}

¹ *Laboratory of Radiation Physics, Belgorod State University, Belgorod, 308015, Russia*

² *John Adams Institute at Royal Holloway, University of London, Egham, TW20 0EX, United Kingdom*

³ *Lebedev Physical Institute, Moscow, 119991, Russia*

* oleynik_a@bsu.edu.ru

ABSTRACT

Lithium niobate (LiNbO₃) single crystal is one of the pyroelectric materials, which can be applicable in energy storage and conversion devices. Theoretical and experimental study of the sinusoidal temperature variation of a single crystal of LiNbO₃ with ultra-low frequency of 1-80 mHz is presented here. The previously unreported phenomenon of the optimal frequency range with maximum amplitude of pyroelectric current oscillations is shown. It is noted that the observed effect is very sensitive to the thermal properties of the material. The impact of thermal properties of the crystal on the optimal frequency range are discussed. The accurate calculations of the pyroelectric coefficient using sinusoidal temperature variation are introduced. The observed phenomenon can be applied in pyroelectric energy converters and storage devices having a cycle time of 10-1000 s.

I. INTRODUCTION

The pyroelectric effect allows to generate electricity changing the temperature of pyroelectric materials¹. This phenomenon makes it possible to design devices for energy conversion and storage^{2,3}, as well as to propose low-power electric generators for several applications, which have become popular in the past years⁴⁻¹³. Another remarkable aspect is the ability to generate a high electric field in vacuum¹⁴. This phenomenon allows us to generate electrons^{15,16}, positive ions¹⁷, X-ray photons^{18,19} and even neutrons^{20,21}. The concepts of a pyroelectric accelerator²² and a deflector of charged particle beams²³ have been developed. These diverse applications of pyroelectricity maintain a strong research interest in the phenomenon discovered quite a long time ago²⁴.

The pyroelectric effect manifests in various forms of materials. For instance, it exhibits in 3D single crystals^{25,26}, ceramics²⁷⁻²⁹, composites³⁰, polymers³¹⁻³³, and in 2D thin films^{34,35}. However, pyroelectricity is the most pronounced in single-domain bulk single crystals, at which the value of the pyroelectric coefficient is the highest compared to the other states of the same material²⁵. One of the most widely used pyroelectric materials is lithium niobate (LiNbO₃, LN), which also exhibits both piezoelectric and ferroelectric properties³⁶. The pyroelectric coefficient of LiNbO₃ varies in the range of $4 - 10 \times 10^{-5}$ C/(m²·°C)^{37,38}, which is very attractive for possible practical applications, such as infrared detectors³⁹, electro-optical devices⁴⁰, charged particle beam control²³, particle generators^{17,19} etc.

The way of temperature change of a pyroelectric material largely determines the electric response. In particular, selection of temperature change rate might sharply increase the X-ray photon yield⁴¹. Sinusoidal temperature variation^{42,43} is a promising regime. This way has proved to be an excellent opportunity to accurately determine the pyroelectric coefficient for samples with a thickness of less than 1 mm at ultra-low oscillation frequencies (tens and hundreds of mHz)^{44,45}. The oscillations with a higher frequency (of the order of 1 kHz) excited in thin films are considered to be efficient energy converters⁴⁶. However, still there is no complete understanding of the pyroelectric effect operation for different oscillation parameters and pyroelectric sample geometries.

This paper provides new information about peculiarities of the pyroelectric response to the temperature variation of lithium niobate in the range of a few to tens of mHz. In particular, it is shown that there are maxima of the amplitudes of both the pyroelectric current oscillations and temperature change

rate. This fact is in good agreement with the classical definition of pyroelectricity and the theory of heat transfer in matter. Nevertheless, previously experimental verification has never been clearly reported. The influence of the thickness and thermal properties of the LN sample on the position of the maximum will be discussed. The ability to accurately determine the pyroelectric coefficient using sinusoidal temperature variation is shown for thicker samples (10 mm). The position of the maximum amplitude of the pyroelectric current can be adjusted. This fact can be useful for the alternating current energy conversion devices.

II. THEORETICAL BACKGROUND

The sinusoidal temperature variation of a pyroelectric sample can be expressed by the following equation⁴²:

$$T(t) = T_0 + T_1 \sin(2\pi\nu t) \quad (1)$$

where T_0 is the initial temperature of the sample, T_1 is the amplitude of temperature oscillations, ν is the frequency. The pyroelectric current is the amount of charge propagated in the closed circuit per unit time during the temperature change. This parameter can be measured by a current meter connected to the circuit. The pyroelectric current can be defined as:

$$i(t) = pA \frac{dT(t)}{dt} \quad (2)$$

where p is the pyroelectric coefficient of the sample, A is the area of the polar surface. For sinusoidal temperature variation, the pyroelectric current can be written as:

$$i(t) = pAT_1 2\pi\nu \cos(2\pi\nu t) \quad (3)$$

Accordingly, the value of amplitude of the pyroelectric current oscillations i_a is defined as:

$$i_a = pAT_1 2\pi\nu \quad (4)$$

From Eqs. (1) and (3) the phase difference between the temperature and the pyroelectric current oscillations is $\pi/2$. The relationship between both types of oscillation is illustrated in Figure 1. The heating phase of the pyroelectric sample (red area) or cooling phase (blue area) corresponds to a certain current polarity determined by the direction of the spontaneous polarization vector. This behaviour is defined by the classical description of the pyroelectric effect¹.

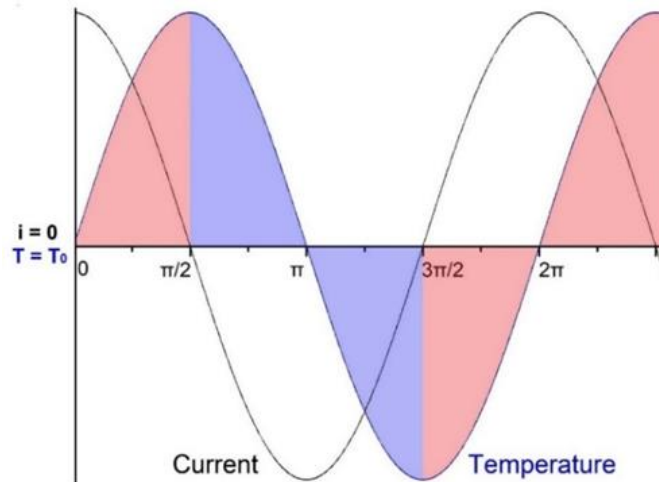


Figure 1. Oscillations of the pyroelectric current (black curve) and temperature of the pyroelectric sample (blue curve) during sinusoidal temperature variation. The red area corresponds to the heating phase, the blue area – to the cooling phase.

The thermal flux can be described by the heat balance equation for a short time interval dt for a thin layer of the sample with a thickness dx . Neglecting the heat loss from the side surfaces^{47,48}:

$$\frac{\partial T(x,t)}{\partial t} = a \frac{\partial^2 T(x,t)}{\partial x^2} \quad (5),$$

where a is the thermal diffusivity of the sample, which characterizes the rate of heat transfer and can be defined as:

$$a = k/C_V \quad (6),$$

where k is the thermal conductivity, C_V is the volumetric heat capacity. The solution of Eq. (5) can be represented as $T(x,t) = T_0 + \theta(x,t)$, where $\theta(x,t)$ is the temperature increment as a result of the heat flux. The $\theta(x,t)$ maximum is equal to the temperature oscillation amplitude T_1 . A particular solution of Eq. (5) is a thermal wave propagating in the pyroelectric sample:

$$\theta(x,t) = T_1 \exp[-(\pi\nu/a)^{1/2}x] \cos[2\pi\nu t - (\pi\nu/a)^{1/2}x] \quad (7)$$

In analogy with Eq. (3) the amplitude of the pyroelectric current oscillations, i_a , from Eq. (4) is proportional to the following expression:

$$i_a \propto 2\pi\nu p A T_1 \exp[-(\pi\nu/a)^{1/2}x] \cos[2\pi\nu t - (\pi\nu/a)^{1/2}x] \quad (8)$$

Eqs. (7) and (8) enable us to consider the dependence of the pyroelectric current amplitude at the $t = \pi$ and the temperature amplitude at $t = \pi/2$ (when the corresponding amplitudes are maximal, see Fig. 1) and for the sample thicknesses of $x = 1, 2, 4, 10$ mm. The calculated dependencies are presented in Fig. 2. The amplitude of temperature oscillations decreases monotonically. An increase in the sample thickness leads to a steeper drop, which can be explained by the influence of the exponential factor in Eq. (7). The amplitude of the pyroelectric current has a maximum appearing due to the superposition of a linear dependence of the pyroelectric current amplitude on frequency and the exponential decay in the temperature oscillation amplitude in Eq. (8). The position of the maximum is determined by the LN sample. A smaller thickness contributes to the weakening of the exponential decay and the optimal frequency shifts upwards. In addition, the maximum of the pyroelectric current has a larger amplitude at a smaller sample thickness. Also, it should be noted that the position of the maximum is very sensitive to the thermal diffusivity, which was taken from Ref. 49 for an optically transparent lithium niobate produced by Crystal Technology and is equal to $a = 1.4 \times 10^{-6}$ m²/s. An increase of thermal diffusivity means an increase of thermal conductivity. Therefore, the pyroelectric current maximum shifts towards higher frequencies with an increase in thermal diffusivity as well. As a result, the presence of a frequency dependence with a maximum amplitude of the pyroelectric current during the sinusoidal temperature variation is predicted theoretically, however it has never been observed experimentally. Note that T_0 has no effect on the presented dependences.

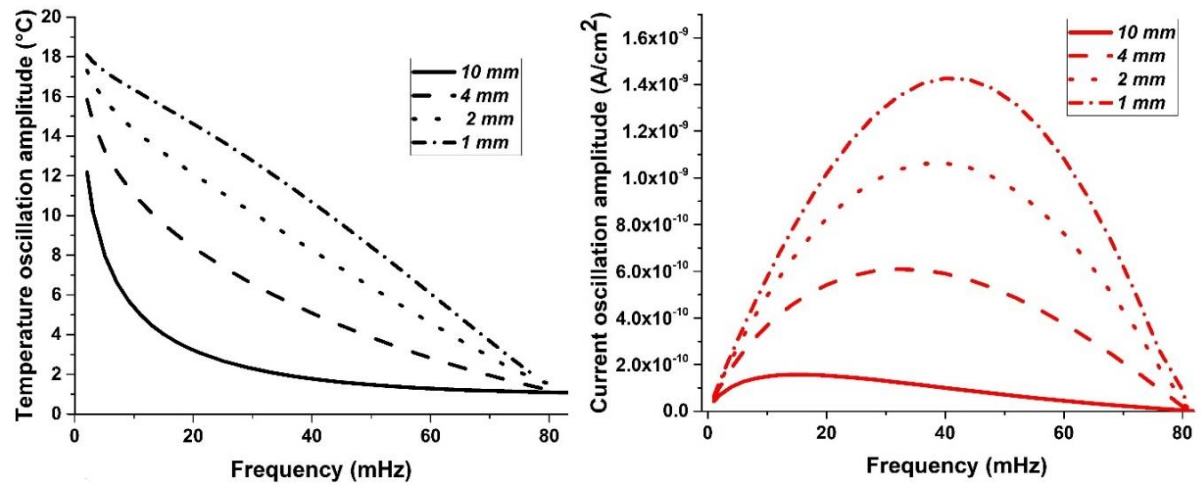


Figure 2. Theoretical dependences of the amplitudes of the temperature oscillations (left, black) and the pyroelectric current (right, red) on frequency.

III. EXPERIMENTAL SETUP

The scheme of the experimental setup is illustrated in Fig. 3. The assembly consisting of LiNbO₃ (LN) crystal, a Peltier element (PE) and a radiator (H) attached to a the bottom surface of the Peltier element was installed inside a metal chamber (C). The Z-surfaces (top and bottom of the LN sample) were covered with aluminium electrodes (E) to ensure a complete charge collection from both surfaces and to close the circuit for measuring the pyroelectric current oscillations using the Keithley 6485 picoammeter (PA). The dimensions of the electrodes were 2 mm wider than the dimensions of the crystal surface. To change the temperature according to Eq. (1) a signal waveform generator (RIGOL DG1062, WG) was used as a power source for the Peltier element. The temperature distribution along the side surfaces of the crystal was contactlessly measured using the FLIR E8 infra-red camera (IC).

A single crystal of lithium niobate (Crystal Technology Inc.) with Z-orientation and different thicknesses of 1, 2, 4, and 10 mm were used in the experiment. The dimensions of Z-surfaces for each sample were 20x20 mm. The Z-surfaces of each sample were polished to a high gloss and showed no visible damage. The LN sample was exposed to low-frequency sinusoidal temperature variation. The minimum variation frequency was 1 mHz. The maximum frequency was determined by the minimum distinguishable temperature variation amplitude (0.25 C). For a sample of 1 mm, the maximum frequency was 80 mHz. With increasing thickness, this value decreased. In each measurement, the power supply parameters of the Peltier element were the same, i.e., the sample was excited by the same thermal regime. T_0 was in the range of 24.5-26 °C in all measurement sets.

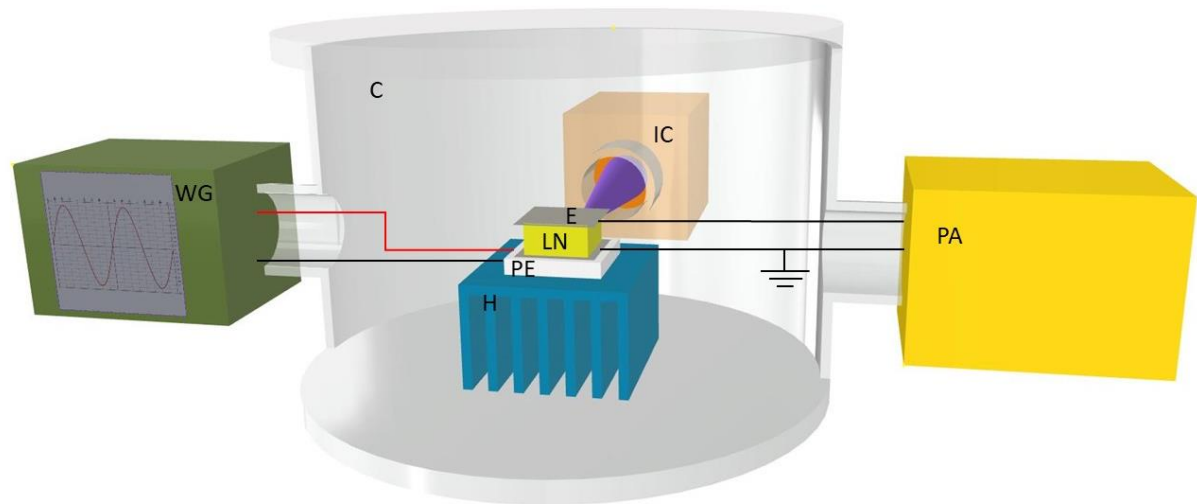


Figure 3. Scheme of the experiment. LN - lithium niobate crystal, PE - Peltier element, E - metal electrodes attached to the polar LN surface, H - radiator, C - metal chamber, IC - infrared camera, WG - waveform generator, PA - picoammeter.

IV. RESULTS AND DISCUSSION

The experimentally obtained amplitudes of temperature and pyroelectric current oscillations as a function of the frequency are shown in Figure 4. The amplitude of temperature oscillations goes down monotonically due to a decrease in the total duration of thermal exposure. We expected the amplitude of temperature oscillations decrease slower, as shown in Fig. 2. However, the shape of the curves is close to an exponential decay. It can be caused by heat losses through side surfaces, which are not taken into account in calculations. The increase in thickness leads to greater impact. A wide maximum of the pyroelectric current amplitude is observed, as predicted by the theoretical calculation. The maximum shifts towards higher frequencies for thinner crystals, as it is noted above. The results are summarized in Table 1. At the same time, it is worth noting that the position of the maximum and the shape of the pyroelectric current curve are also quite different from the theoretical calculation.

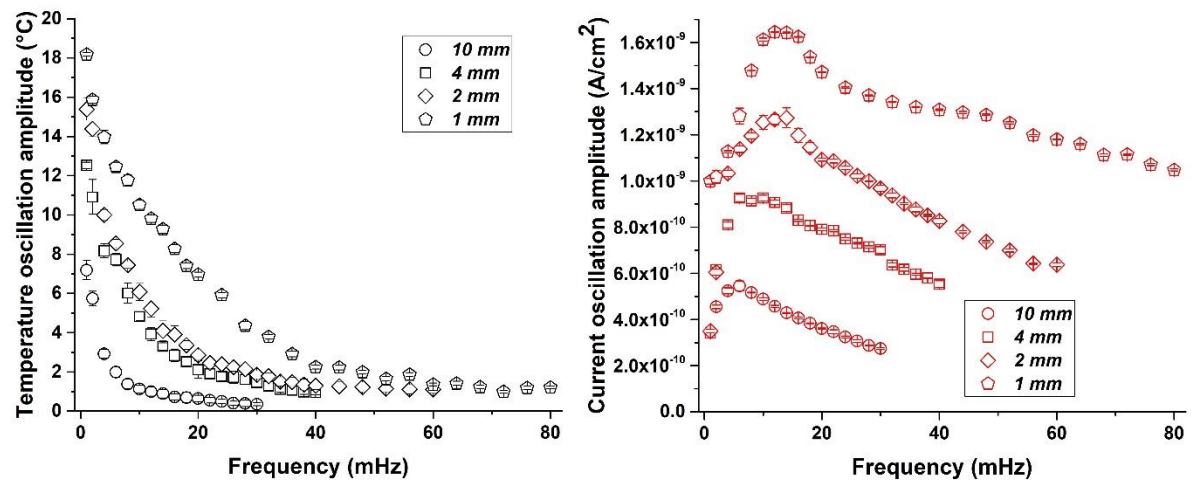


Figure 4. Experimentally obtained amplitudes of temperature oscillations (left, black) and pyroelectric current oscillations (right, red) versus frequency for lithium niobate samples with different thicknesses.

Table 1. Position of the maximum amplitude of the pyroelectric current oscillations for lithium niobate samples with different thickness.

Sample thickness (mm)	Position of the maximum amplitude, experiment (mHz)	Position of the maximum amplitude, calculation (mHz), $a = 1.4 \times 10^{-6}$ m ² /s	Position of the maximum amplitude, calculation (mHz), $a = 1.0 \times 10^{-7}$ m ² /s
1	14±2	42	12
2	12±2	40	11
4	8±2	32	9
10	6±1	16	6

The value of the thermal diffusivity a has a strong influence on the shape of the frequency dependence. Figure 5 presents a comparison of the obtained experimental data for the sample of 1 mm with a theoretical calculation at $a = 1.4 \times 10^{-6}$ m²/s from Ref 49 and with a selected value of $a = 1.0 \times 10^{-7}$ m²/s. A significant decrease in the thermal diffusivity (by a factor of 14) makes it possible to qualitatively reproduce experimental dependence by theoretical calculations for samples with smaller thickness. The values of the thermal diffusivity for our samples are not available, but there are evidences of such low

values of a ⁵⁰, which is determined by the conditions of the crystal growth. For other thicknesses, we observe a similar picture, when the calculation agrees well with the experiment at the value of $a = 0.9 - 1.3 \times 10^{-7} \text{ m}^2/\text{s}$. Hence, some disagreement between the experiment and the theoretical calculation may be due to the lower value of the thermal diffusivity of used samples. Finally, we can state that experimental dependences of temperature and pyroelectric current oscillations can be described theoretically from the heat balance equation and the classical description of the pyroelectric effect.

The thermal diffusivity depends rather strongly on the sample temperature⁴⁹. Fig. 4 in Ref. 49 shows the dependence of the thermal diffusivity of lithium niobate on temperature. Now we can estimate the contribution of thermal properties on optimal frequency range. Calculated optimal frequency dependence (at which the amplitude of the pyroelectric current is maximal) on the thickness and temperature of the sample is illustrated in Figure 6. This dependence does not include the change in the pyroelectric coefficient with increase in temperature. Also, it is implied that the amplitude of temperature oscillation is quite small (as in our experiment), that we can exclude the impact the change of pyroelectric coefficient during oscillations. The optimal frequency goes down with an increase in temperature. However, above 200 °C this change is already insignificant and the position of the optimal frequency can be considered to be constant. At room temperatures, this effect can lead to smearing and shifting the optimal frequency. It is apparent that thinner samples are more preferable due to even weaker dependence. For example, the optimal frequencies for 1- and 2-mm thick samples are very close for all temperatures.

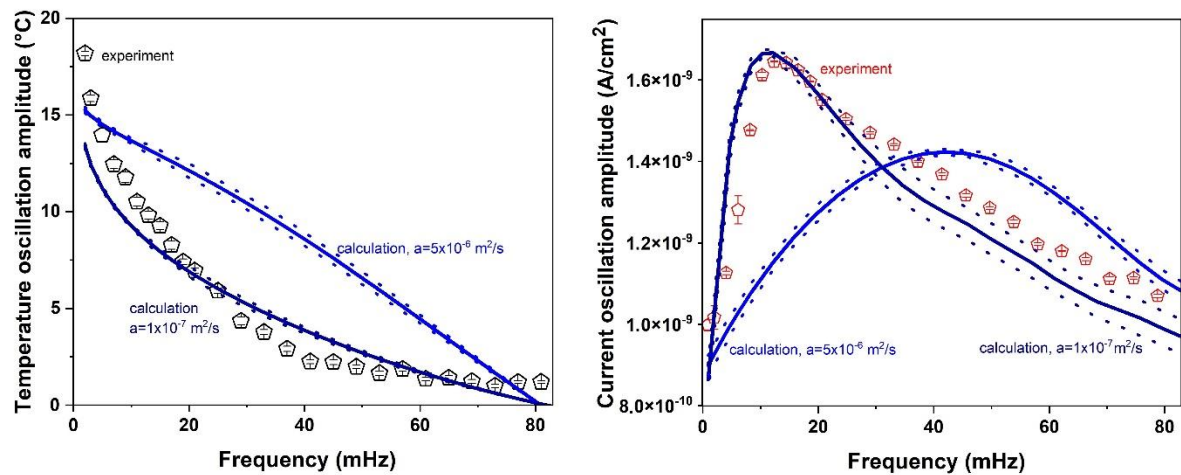


Figure 5. Comparison of the experimental dependences of the amplitude of temperature oscillations and pyroelectric current oscillations on frequency with the theoretical calculation at the value of the thermal diffusivity $a = 1.4 \times 10^{-6} \text{ m}^2/\text{s}$ from Ref. 49 and at the selected value $= 1.0 \times 10^{-7} \text{ m}^2/\text{s}$ for a sample of 1 mm thick.

The temperature change rate can have a rather large effect on the manifestation of the pyroelectric effect⁴¹. Figure 7 presents the temperature change rate at the moment of the maximum amplitude of the pyroelectric current (at this point, the temperature change rate should be maximal) for different variation frequencies and the LN sample thickness. There is a certain correlation with the frequency dependence of the pyroelectric current amplitude. In particular, the positions of the maxima of both dependencies coincide. This is quite understandable, since the pyroelectric current and the temperature change rate are directly proportional to each other⁴¹, as it follows from Eq. (2). Thereby, the maximum temperature change rate increases with the oscillation frequency up to a certain limit determined by the thermal constants of the pyroelectric sample.

A sinusoidal temperature variation has been shown to be an excellent way to accurately determine the pyroelectric coefficient⁴⁴. Figure 8 illustrates the frequency dependence of the pyroelectric coefficient calculated from the experiment for a sample with a thickness of 10 mm. The spread of the pyroelectric coefficient obtained in all measurements does not exceed 7%. The average value within measurement uncertainty is $(7.67 \pm 0.09) \times 10^{-5} \text{ C}/(\text{m}^2 \times ^\circ\text{C})$, which is fairly consistent with the passport value of $7.80 \times 10^{-5} \text{ C}/(\text{m}^2 \times ^\circ\text{C})$.

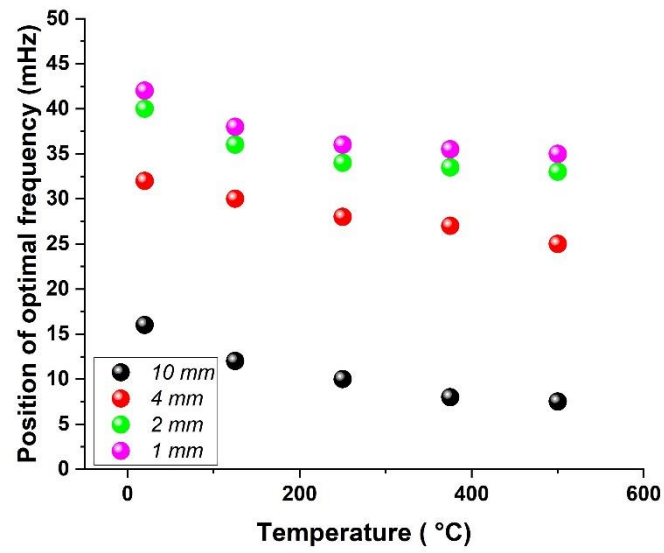


Figure 6. Position of the optimal temperature variation frequency for a lithium niobate sample as a function of temperature for different thicknesses based on temperature dependence of thermal diffusivity from Ref [49].

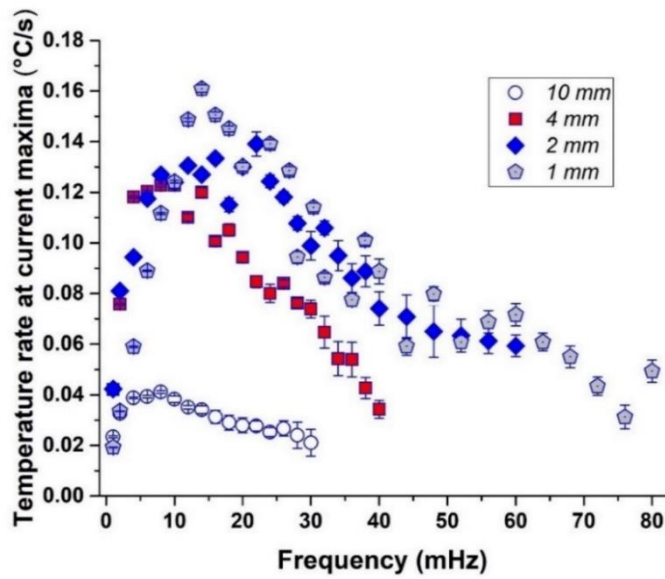


Figure 7. Dependence of the temperature change rate at the moment of the pyroelectric current oscillation extremum on the variation frequency and sample thickness.

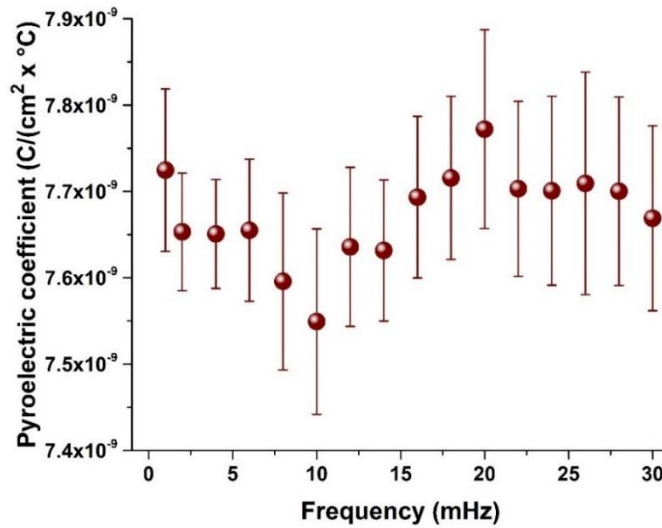


Figure 8. Pyroelectric coefficient versus frequency for a 10 mm thick lithium niobate sample.

V. CONCLUSION

The pyroelectric response of a single crystal of lithium niobate to a sinusoidal temperature variation with a frequency from a few to tens of mHz has been comprehensively studied. It has been shown that there is a frequency maximum of the pyroelectric current oscillation amplitude. This maximum follows from the solution of the heat balance equation and the definition of the pyroelectric effect. The position of pyroelectric current amplitude maximum and shape of the dependence are determined by the thickness of the pyroelectric sample and its thermal constants (thermal diffusivity). The maximum shifts towards higher frequencies with a decrease in the thickness, which is consistent with the theoretical calculation. The maximum temperature change rate also has a maximum that coincides with the amplitude of the pyroelectric current.

Based on early work⁴⁹ on measuring the temperature dependence of the thermal diffusivity, it is expected that the optimal frequency range (at which the amplitude of the pyroelectric current is maximum) should shift towards lower frequencies with an increase of the temperature. However, this effect is rarely noticeable for samples of large thickness (about 10 mm) and at around ambient temperature. Note that our work also confirms the possibility of accurate determination of the pyroelectric coefficient applying sinusoidal temperature variation.

The discovered phenomenon of optimal frequency range with a maximum of pyroelectric current can be useful for energy converters and storage devices having a cycle time of 10-1000 s. Selection of a sample with a certain thickness and thermal diffusivity allows to reach more efficient conversion of heat into electricity. A very curious continuation of this work would be to study the electron emission and the electric field generation in the same way, i.e., sinusoidal temperature variation. It can be perspective in the development of more efficient pyroelectric accelerators, as well as sources and deflectors of particle beams. In conclusion, we note that the discussed effect shows a deep relationship between the thermal and electrical properties of pyroelectric materials, as well as the need for a more careful control of the thermal excitation process.

ACKNOWLEDGEMENTS

The work was financially supported by a Program of the Ministry of Education and Science of the Russian Federation for higher education establishments, project No. FZWG-2020-0032 (2019-1569). The work of P.K. was supported by Science and Technology Facilities Council via John Adams Institute for Accelerator Science at Royal Holloway, University of London (Grant Ref: ST/V001620/1).

REFERENCES

- ¹ S. Lang, *Sourcebook of Pyroelectricity* (Gordon and Breach, London, 1974).
- ² R.W. Whatmore, Rep. Prog. Phys. **49**, 1335 (1986).
URL: <https://iopscience.iop.org/article/10.1088/0034-4885/49/12/002>
- ³ M.H. Lee, R. Guo, A.S. Bhalla, J. Electroceramics **2**, 229 (1998).
URL: <https://link.springer.com/article/10.1023/A%3A1009922522642>
- ⁴ S.K.T. Ravindran, T. Huesgen, M. Kroener, P. Woias, Appl. Phys. Lett. **99**(10), 104102 (2011).
URL: <https://aip.scitation.org/doi/abs/10.1063/1.3633350>
- ⁵ D. Zabek, J. Taylor, V. Ayel, Y. Bertin, C. Romestant and C.R. Bowen, J. Appl. Phys. **120**(2), 024505 (2016).
URL: <https://aip.scitation.org/doi/abs/10.1063/1.4958338>
- ⁶ T. Zhao, W. Jiang, H. Liu, D. Niu, X. Li, W. Liu, X. Lu, B. Chen, Y. Shi, L. Yin, B. Lu, Nanoscale **8**(15), 8111 (2016).
URL: <https://pubs.rsc.org/en/content/articlelanding/2016/nr/c5nr09290f>
- ⁷ A. Sultana, M. M. Alam, T. R. Middy and D. Mandal, Appl. Energy **221**, 299 (2018).
URL: <https://ideas.repec.org/a/eee/appene/v221y2018icp299-307.html>
- ⁸ A. Thakre, A. Kumar, H.C. Song, D.Y. Jeong, J. Ryu, Sensors **19**(9), 2170 (2019).
URL: <https://www.mdpi.com/1424-8220/19/9/2170>
- ⁹ J. Kim, S. Yamanaka, I. Murayama, T. Katou, T. Sakamoto, T. Kawasaki, T. Fukuda, T. Sekino, T. Nakayma, M. Takeda, M. Baba, H. Tanaka, K. Aizawa, H. Hashimoto and Y. Kim, Sustainable Energy & Fuels **4**(3), 1143 (2020).
URL: <https://pubs.rsc.org/en/content/articlelanding/2020/se/c9se00283a>
- ¹⁰ X. Kang, S. Jia, R. Xu, S. Liu, J. Peng, H. Yu and X. Zhou, Nano Energy **88**, 106245 (2021).
URL: <https://www.sciencedirect.com/science/article/abs/pii/S2211285521005000>
- ¹¹ G. Clementi, G. Lombardi, S. Margueron, M. Angel Suarez, E. Lebrasseur, S. Ballandras, J. Imbaud, F. Lardet-Vieudrin, L. Gauthier-Manuel, B. Dulmet, M. Lallart, A. Bartasyle, Mech. Systems and Signal Proc. **149**, 107171 (2021).
URL: <https://doi.org/10.1016/j.ymsp.2020.107171>
- ¹² G. Clementi, M. Ouhabaz, S. Margueron, M. A. Suarez, F. Bassignot, L. Gauthier-Manuel, D. Belharet, B. Dulmet, A. Bartasyle, Appl. Phys. Lett. **119**, (2021) 013904
URL: <https://doi.org/10.1063/5.0052615>
- ¹³ G. Barrientos, G. Clementi, C. Trigona, M. Ouhabaz, L. Gauthier-Manuel, D. Belharet, S. Margueron, A. Bartasyle, G. Malandrino, S. Baglio Sensors **22**, (2022) 559.
URL: <https://doi.org/10.3390/s22020559>
- ¹⁴ V. Sandomirsky, Y. Schlesinger, R. Levin, J. Appl. Phys. **100**(11), 113722 (2006).
URL: <https://aip.scitation.org/doi/abs/10.1063/1.2399306>
- ¹⁵ J.D. Brownridge, S. M. Shafroth., Appl. Phys. Lett. **79**, 3364 (2001).
URL: <https://aip.scitation.org/doi/10.1063/1.1418458>
- ¹⁶ N. Kukhtarev, T. Kukhtareva, M. Bayssie, J. Wang and J.D. Brownridge, J. Appl. Phys. **96**, 6794 (2004).
URL: <https://aip.scitation.org/doi/abs/10.1063/1.1808479>
- ¹⁷ J.A. Geuther and Y. Danon, J. Appl. Phys. **97**(7), 074109 (2005).
URL: <https://aip.scitation.org/doi/abs/10.1063/1.1884252>
- ¹⁸ J.D. Brownridge, Nature **358**, 287 (1992).
URL: <https://www.nature.com/articles/358287b0>
- ¹⁹ J.A. Geuther and Y. Danon, J. Appl. Phys. **97**(10), 104916 (2005).
URL: <https://aip.scitation.org/doi/abs/10.1063/1.1915536>
- ²⁰ B. Naranjo, J. Gimzewski, S. Putterman, Nature **434**, 1115 (2005).
URL: <https://www.nature.com/articles/nature03575>
- ²¹ W. Tornow, J.D. Brownridge, S. M. Shafroth, J. Appl. Phys. **104**(3), 034905 (2008).
URL: <https://aip.scitation.org/doi/abs/10.1063/1.2963190>
- ²² T.Z. Fullem and Y. Danon, J. Appl. Phys. **106**(7), 074101 (2009).

URL: <https://aip.scitation.org/doi/full/10.1063/1.3225916>

²³ A.N. Oleinik, A.S. Kubankin, R.M. Nazhmudinov, K.A. Vokhmyanina, A.V. Shchagin and P.V. Karataev, *JINST* **11**, P08007 (2016).

URL: <https://iopscience.iop.org/article/10.1088/1748-0221/11/08/P08007>

²⁴ D. Bruster, *Edinburgh J. Sci.* **7**, 231 (1824).

²⁵ M. Lines, A. Glass, *Principles and applications of ferroelectrics and related materials* (Clarendon Press, Oxford, 1979).

²⁶ B. Yacobi, Y. Brada, *J. Appl. Phys.* **47(4)**, 1243 (1976).

URL: <https://aip.scitation.org/doi/10.1063/1.322768>

²⁷ S.A.M. Tofail, C. Baldisserri, D. Haverty, J. B. McMonagle, J. Erhart, *J. Appl. Phys.* **106(10)**, 106104 (2009).

URL: <https://aip.scitation.org/doi/10.1063/1.3262628>

²⁸ S.T. Lau, C.H. Cheng, S.H. Choy, D.M. Lin, K.W. Kwok, H.L.W. Chan, *J. Appl. Phys.* **103(10)**, 104105 (2008).

URL: <https://aip.scitation.org/doi/10.1063/1.2927252>

²⁹ A. Levstik, B. Golob, M. Kosec, *J. Appl. Phys.*, **71(8)**, 3922 (1992).

URL: <https://aip.scitation.org/doi/10.1063/1.350861>

³⁰ K.-H. Chew, F.G. Shin, B. Ploss, H.L.W. Chan and C.L. Choy, *J. Appl. Phys.* **94**, 1134 (2003).

URL: <https://aip.scitation.org/doi/10.1063/1.1583154>

³¹ T. Furukawa, *IEEE Trans. On Electric. Ins.* **24(3)**, 375 (1989).

URL: <https://ieeexplore.ieee.org/document/30878>

³² J. J. Crosnier, F. Micheron, G. Dreyfus, J. Lewiner, *J. Appl. Phys.* **47(11)**, 4798 (1976).

URL: <https://aip.scitation.org/doi/10.1063/1.322519>

³³ R.E. Salomon, H. Lee, C.S. Bak, M.M. Labes, *J. Appl. Phys.* **47(9)**, 4206 (1976).

URL: <https://aip.scitation.org/doi/10.1063/1.323291>

³⁴ J.D. Zook and S.T. Liu, *J. Appl. Phys.*, **49(8)**, 4604 (1978).

URL: <https://aip.scitation.org/doi/10.1063/1.325442>

³⁵ E.A. Eliseev, N.V. Morozovsky, M.Y. Yeliseiev, A.N. Morozovska, *J. Appl. Phys.* **120(17)**, 174102 (2016).

URL: <https://aip.scitation.org/doi/10.1063/1.4966611>

³⁶ R.S. Weis, T.K. Gaylord, *Appl. Phys. A* **37(4)**, 191 (1985).

URL: <https://link.springer.com/article/10.1007/BF00614817>

³⁷ A. Savage, *J. Appl. Phys.* **37(8)**, 3071 (1966).

URL: <https://aip.scitation.org/doi/10.1063/1.1703164>

³⁸ S.T. Popescu, A. Petris, V.I. Vlad, *J. Appl. Phys.* **113(4)**, 043101 (2013).

<https://aip.scitation.org/doi/10.1063/1.4788696>

³⁹ S.L. Bravina, N.V. Morozovsky, A.N. Morozovska, S. Gille, J.-P. Salvestrini, M.D. Fontana, *Ferroelectrics* **353**, 636 (2007).

URL: <https://www.tandfonline.com/doi/abs/10.1080/00150190701368166?journalCode=gfer20>

⁴⁰ M. Li, J. Ling, Y. He, U.A. Javid, S. Xue and Q. Lin, *Nat Commun* **11**, 4123 (2020).

URL: <https://www.nature.com/articles/s41467-020-17950-7>

⁴¹ A.S. Kubankin, A.S. Chepurinov, O.O. Ivashchuk, V.Yu. Ionidi, I.A. Kishin, A.A. Klenin, A.N. Oleinik and A.V. Shchagin, *AIP Advances* **8**, 035207 (2018).

URL: <https://aip.scitation.org/doi/full/10.1063/1.5006486>

⁴² L.E. Garn, E.J. Sharp, *J. Appl. Phys.* **53** 8974 (1982).

URL: <https://aip.scitation.org/doi/10.1063/1.330454>

⁴³ L.E. Garn, E.J. Sharp, *J. Appl. Phys.* **53** 8980 (1982).

URL: <https://aip.scitation.org/doi/10.1063/1.330455>

⁴⁴ H. Khanbareh, J.B.J. Schelen, S. van der Zwaag, W.A. Groen, *Rev. Sci. Instrum.* **86** 105111 (2015).

URL: <https://aip.scitation.org/doi/full/10.1063/1.4932678>

⁴⁵ G. Gerlach, G. Suchanek, A. Movchikova, O. Malyshkina, *Proc. of SPIE* **6530** 65300B-1 (2007).

This is the author's peer reviewed, accepted manuscript. However, the online version of record will be different from this version once it has been copyedited and typeset.
PLEASE CITE THIS ARTICLE AS DOI: 10.1063/1.5124599

URL: <https://doi.org/10.1117/12.715534>

⁴⁶ B. Bhatia, A.R. Damodaran, H. Cho, L.W. Martin, W.P. King, J. Appl. Phys. **116**(19), 194509 (2014).

URL: <https://aip.scitation.org/doi/abs/10.1063/1.4901993>

⁴⁷ B.-D. Ni, Int. J. Heat and Mass Transfer **116**, 314 (2018).

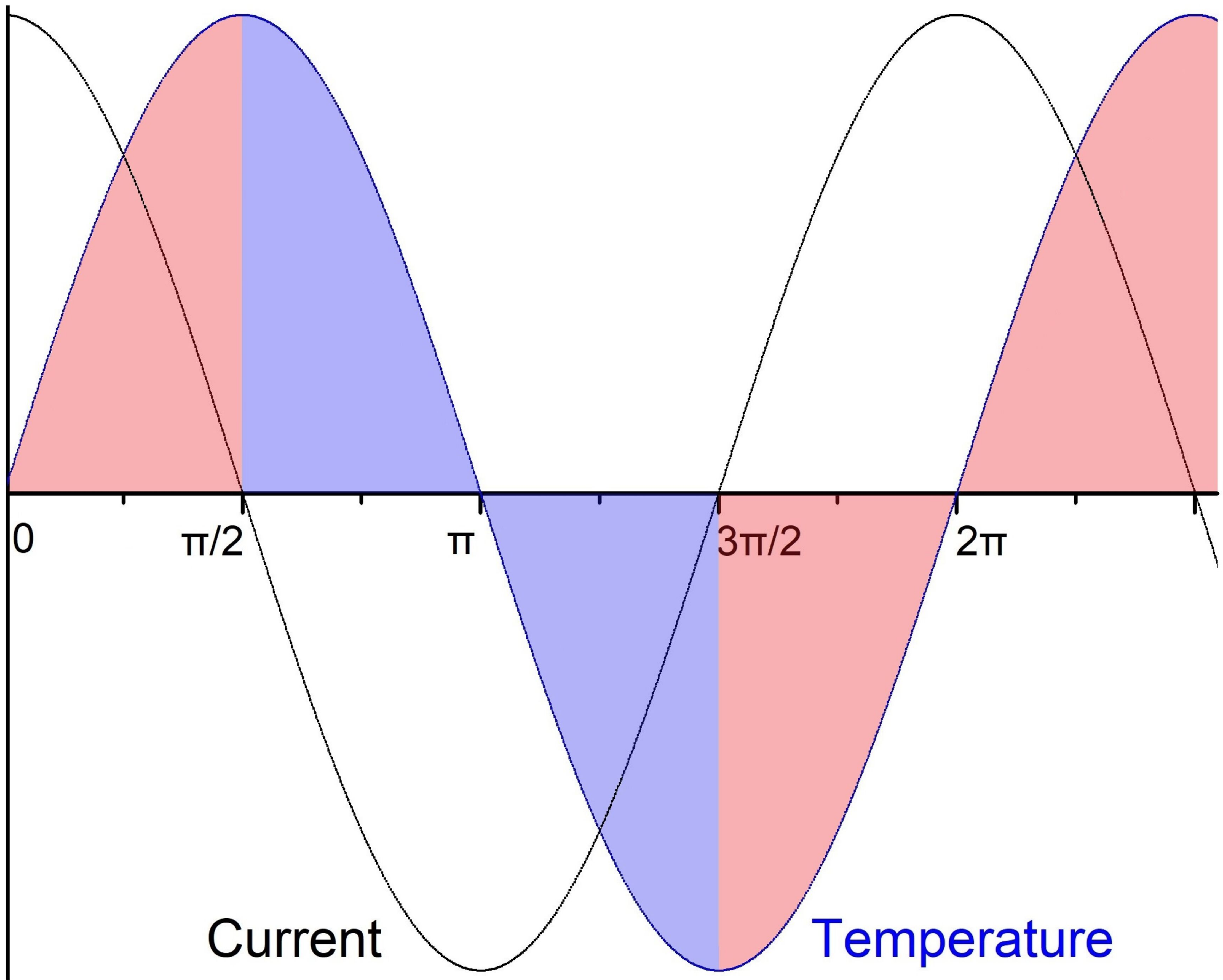
URL: <https://www.sciencedirect.com/science/article/abs/pii/S0017931017330508?via%3Dihub>

⁴⁸ A. Bush, *Pyroelectric effect and its applications*, (In Russian), (MIREA, Moscow, 2005).

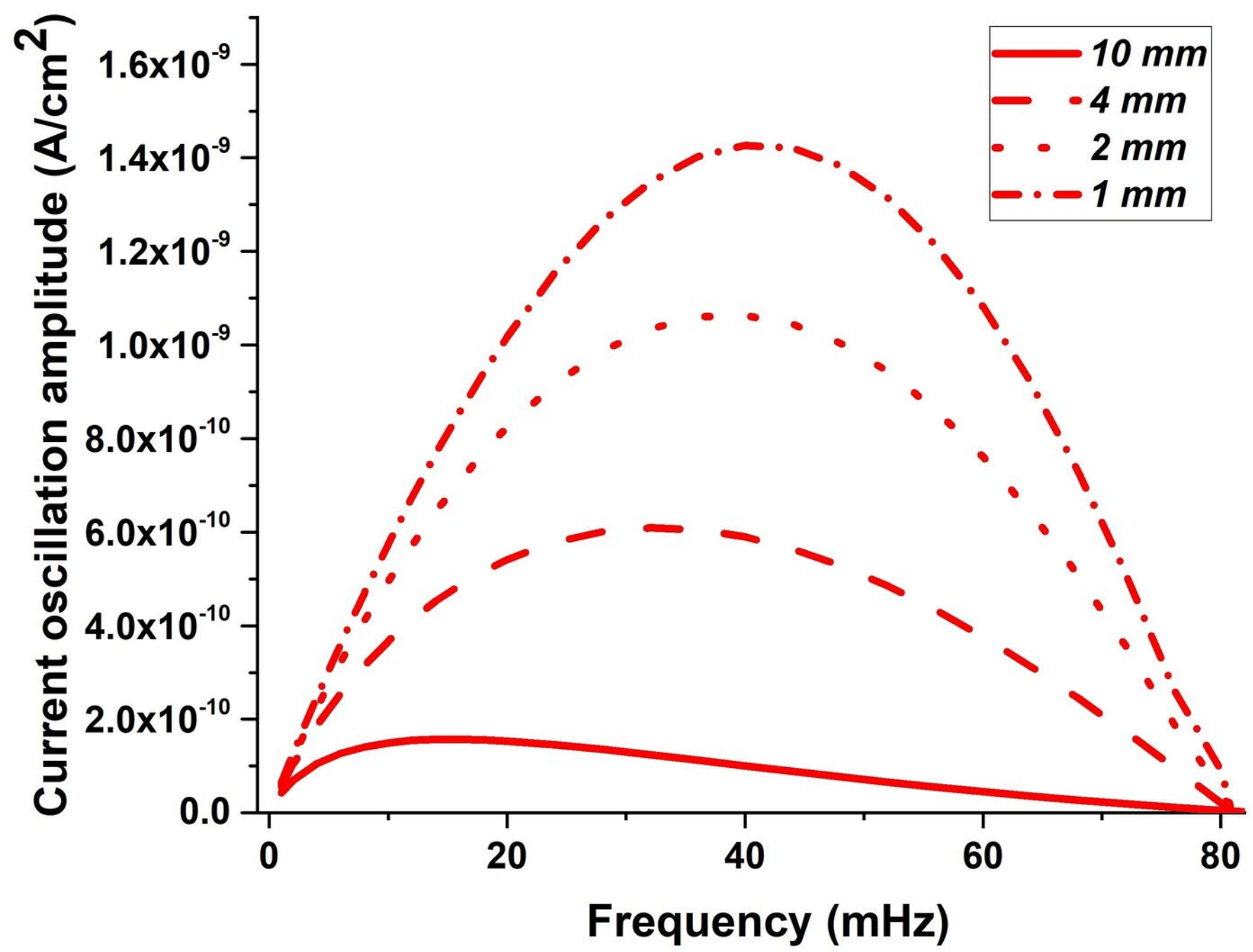
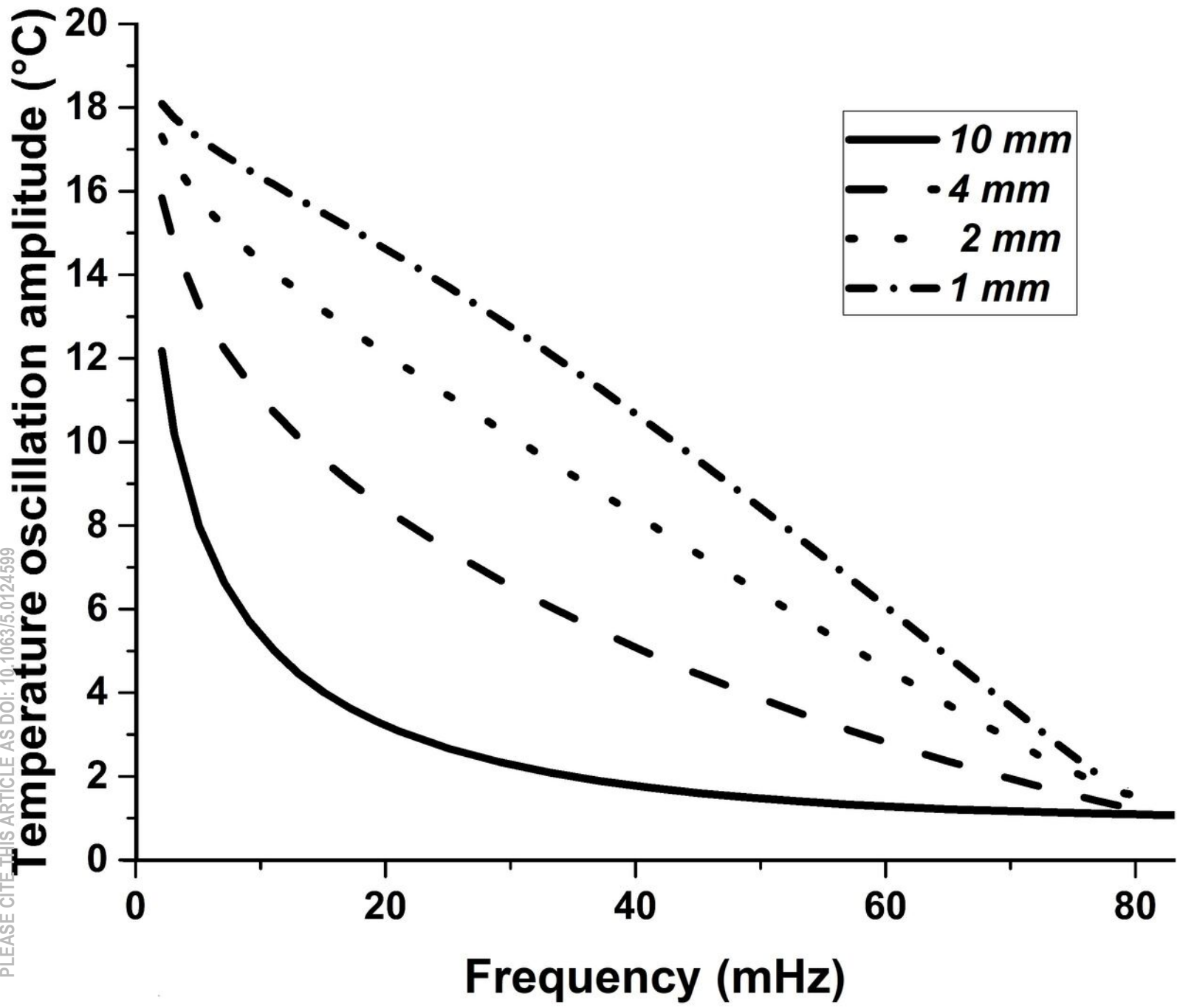
⁴⁹ R.A. Morgan, K.I. Kang, C.C. Hsu, C.L. Koliopoulos, N. Peyghambarian, Appl. Opt. **26** (24) 5266 (1987).

URL: <https://opg.optica.org/ao/abstract.cfm?uri=ao-26-24-5266>

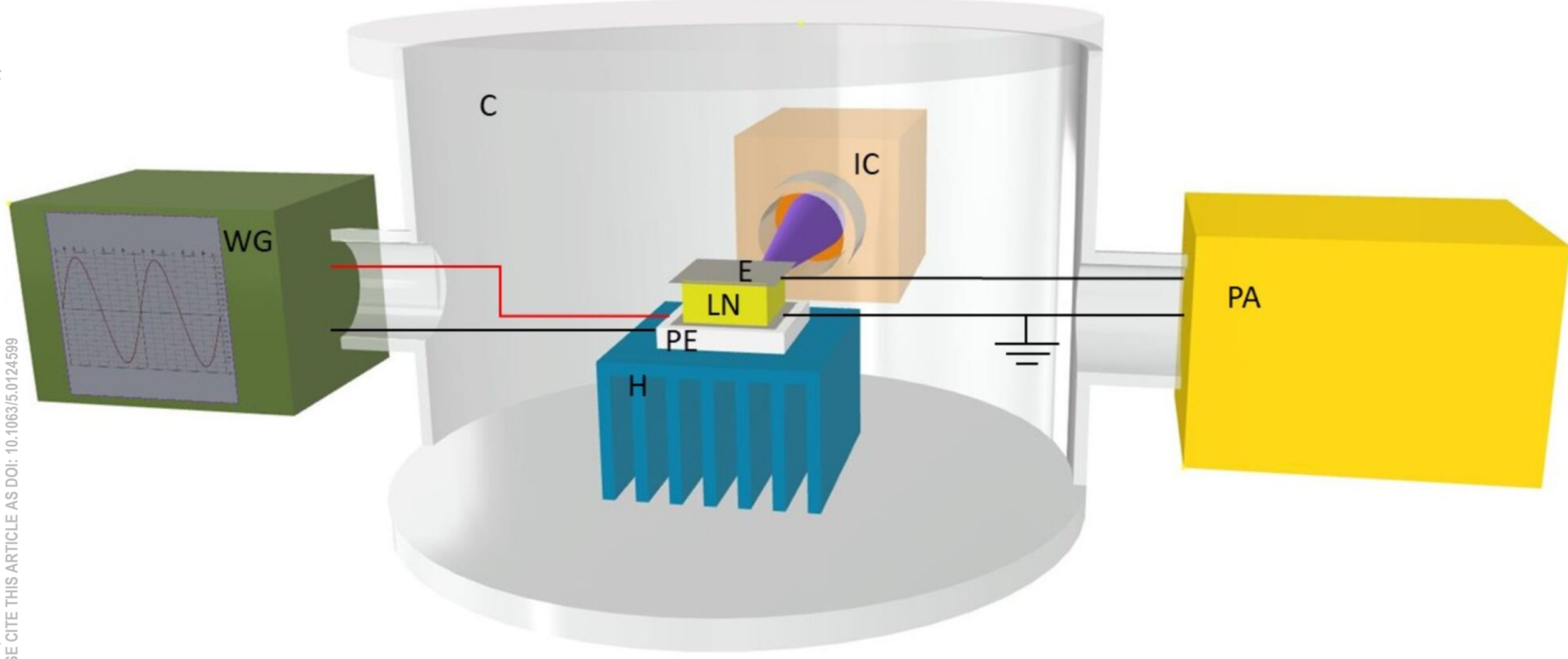
$$\mathbf{i} = \mathbf{0}$$
$$\mathbf{T} = \mathbf{T}_0$$



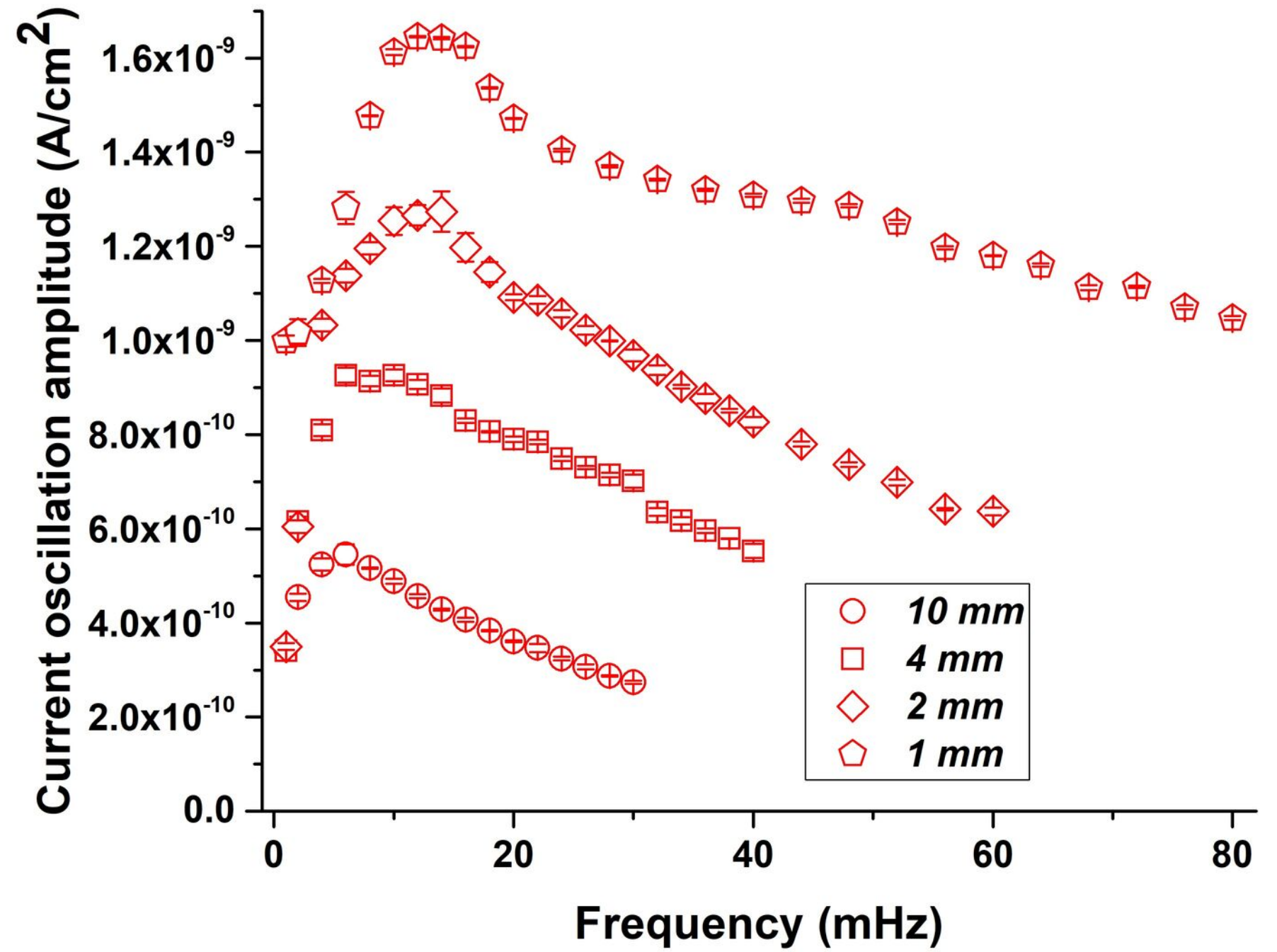
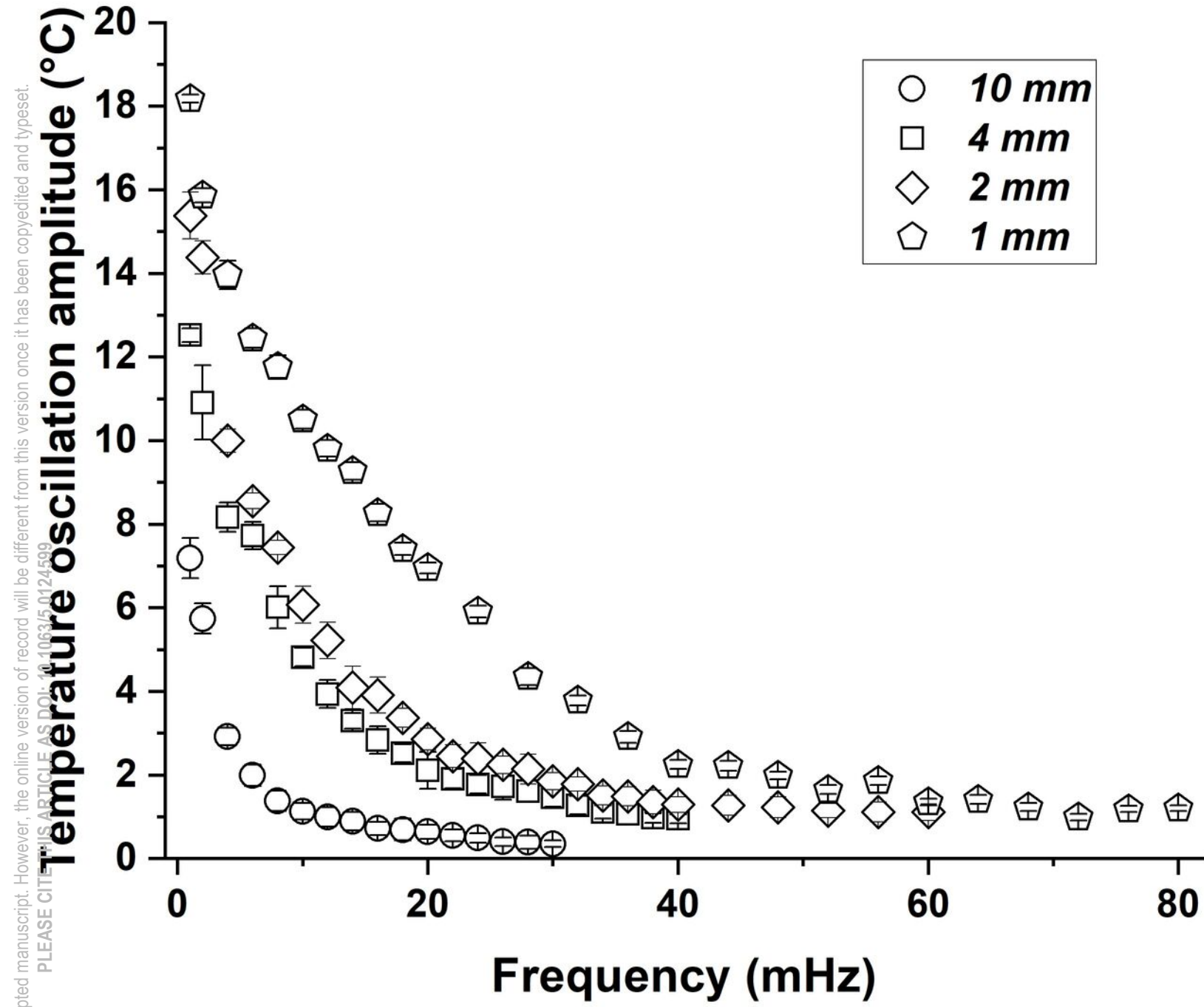
This is the author's peer reviewed, accepted manuscript. However, the online version of record will be different from this version once it has been copyedited and typeset.
PLEASE CITE THIS ARTICLE AS DOI: 10.1063/5.0124599



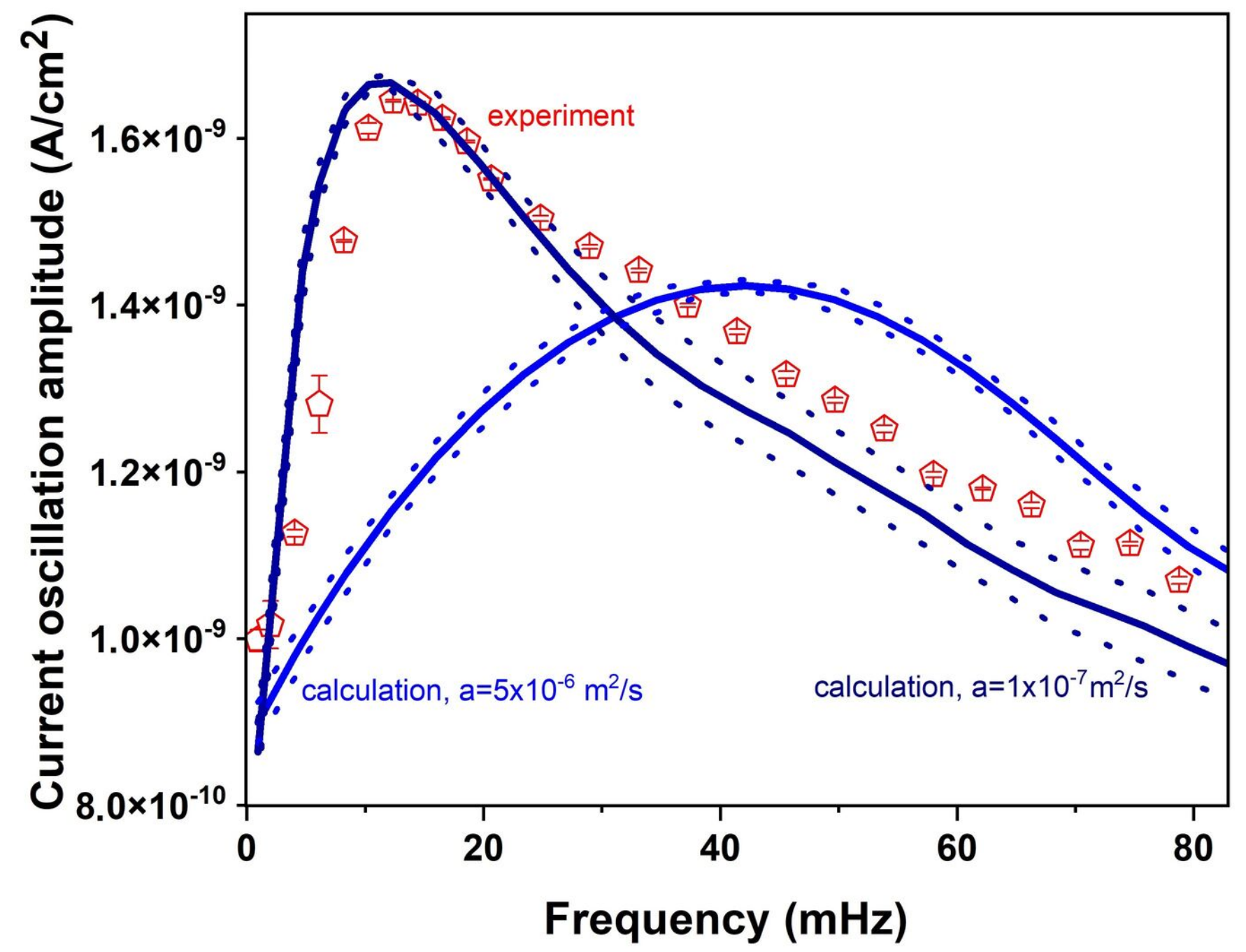
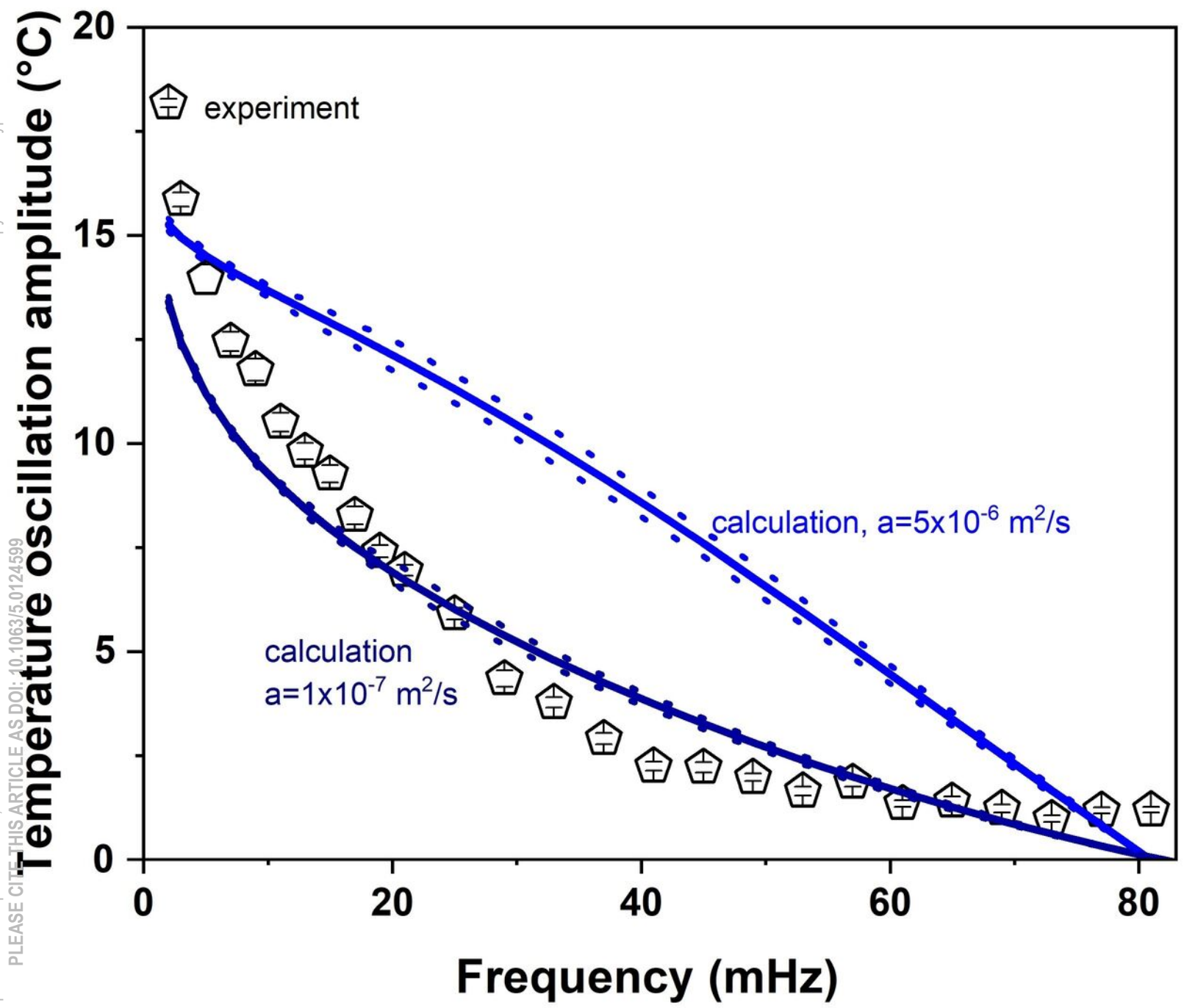
This is the author's peer reviewed, accepted manuscript. However, the online version of record will be different from this version once it has been copyedited and typeset.
 PLEASE CITE THIS ARTICLE AS DOI: 10.1063/5.0124599



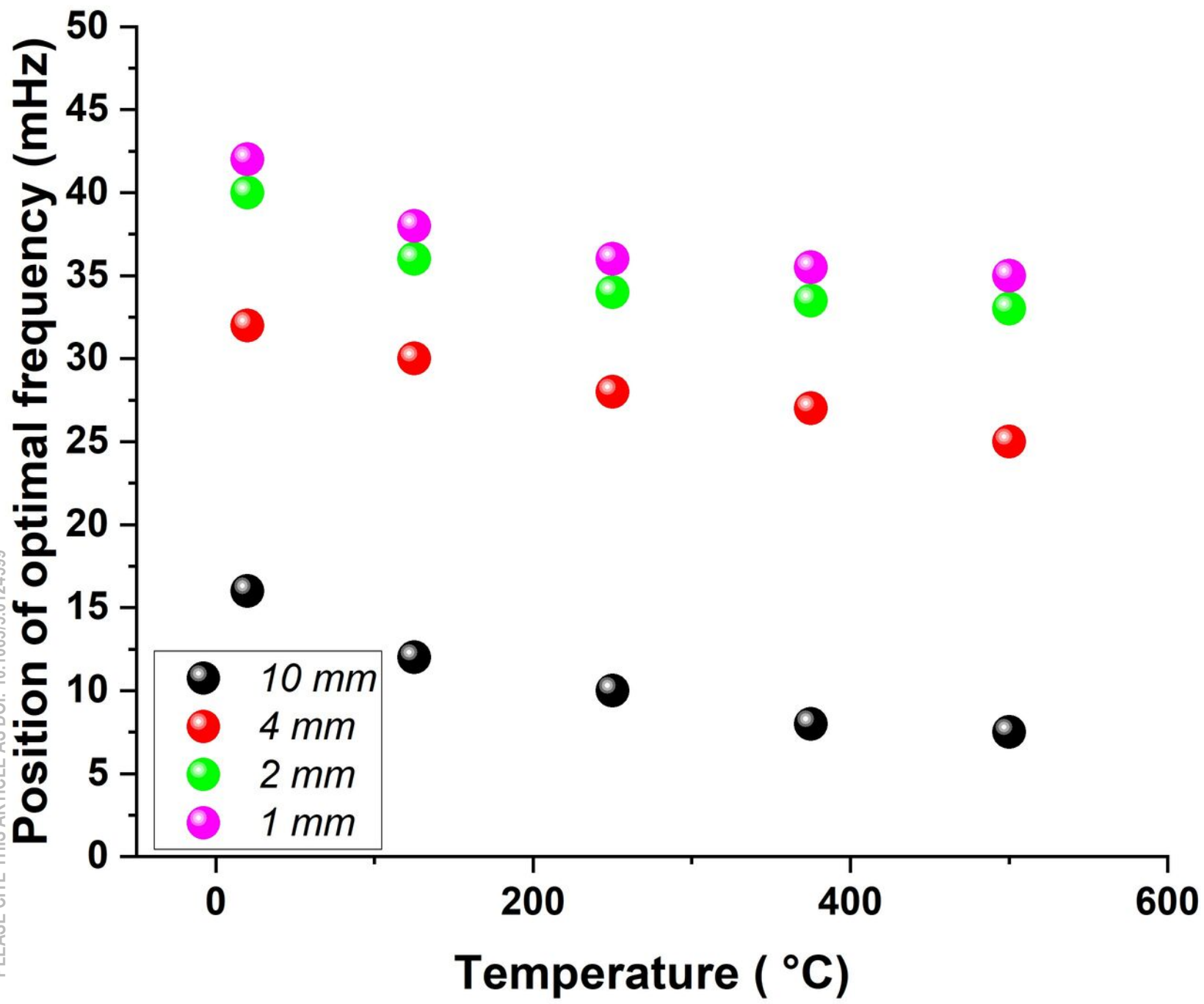
This is the author's peer reviewed, accepted manuscript. However, the online version of record will be different from this version once it has been copyedited and typeset.
PLEASE CITING THIS ARTICLE AS DOI: 10.1063/1.5012459



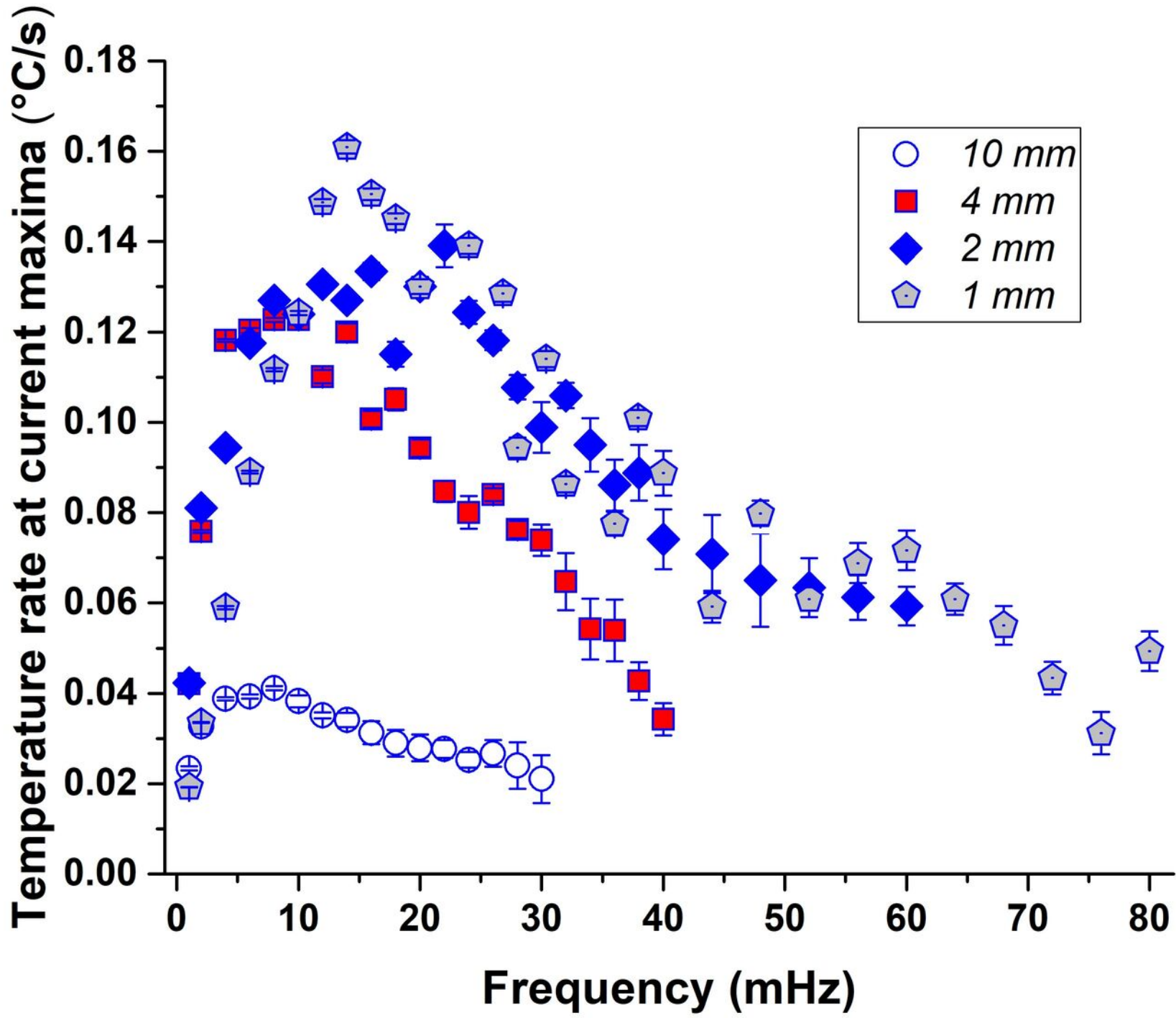
This is the author's peer reviewed, accepted manuscript. However, the online version of record will be different from this version once it has been copyedited and typeset. PLEASE CITE THIS ARTICLE AS DOI: 10.1063/5.0124599



This is the author's peer reviewed, accepted manuscript. However, the online version of record will be different from this version once it has been copyedited and typeset.
PLEASE CITE THIS ARTICLE AS DOI: 10.1063/5.0124599



This is the author's peer reviewed, accepted manuscript. However, the online version of record will be different from this version once it has been copyedited and typeset.
PLEASE CITE THIS ARTICLE AS DOI: 10.1063/5.0124599



This is the author's peer reviewed, accepted manuscript. However, the online version of record will be different from this version once it has been copyedited and typeset.
PLEASE CITE THIS ARTICLE AS DOI: 10.1063/5.0124599

